

A dense gas survey of the gamma-ray sources HESS J1731–347 and HESS J1729–345

Nigel Maxted^{*a}, Gavin Rowell^b, Phoebe de Wilt^b, Michael Burton^c, Matthieu Renaud^a, Yasuo Fukui^d, Jarryd Hawkes^b, Rebecca Blackwell^b, Fabien Voisin^b, Vicki Lowe^{ce} and Felix Aharonian^f

^aLaboratoire Univers et Particules de Montpellier, Université de Montpellier 2, France

^bSchool of Chemistry and Physics, University of Adelaide, Adelaide, Australia

^cSchool of Physics, University of New South Wales, Sydney, Australia

^dDepartment of Astrophysics, Nagoya University, Japan

^eAustralia Telescope National Facility, CSIRO Astronomy and Space Science, Australia

^fMax-Planck-Institut für Kernphysik, Heidelberg, Germany

E-mail: nigel.maxted@univ-montp2.fr

The results of Mopra molecular spectral line observations towards the supernova remnant HESS J1731–347 (G353.6–0.7) and the unidentified gamma-ray source HESS J1729–345 are presented. Dense molecular gas in three different velocity-bands (corresponding to three Galactic arms) are investigated using the CS(1-0) line. The CS-traced component provides information about the dense target material in a hadronic scenario for gamma-ray production (cosmic-rays interacting with gas) and an understanding of the dynamics. Furthermore, the effects of cosmic ray diffusion into dense gas may alter the gamma-ray spectrum to cause a flattening of spectra towards such regions. Dense molecular gas mass at a level of $\sim 10^5 M_{\odot}$ was revealed in this survey, with mass of the order of $\sim 10^3 M_{\odot}$ towards HESS J1729–345 in each coincident Galactic arm, but no significant detection of dense molecular gas towards HESS J1731–347 at the currently-preferred distance of ~ 5.2 - 6.2 kpc was discovered.

Cosmic Rays and the InterStellar Medium

24-27 June 2014

Montpellier, France

*Speaker.

1. Introduction

HESS J1731–347 is a TeV gamma-ray source (Aharonian et al., 2008; Abramowski et al., 2011) associated with the shell-type supernova remnant (SNR), G353.6–0.7 (Tian et al., 2008). The nature of the nearby gamma-ray source HESS J1729–345 (north of HESS J1731–347, see Figure 1) has remained unclear since being resolved as a separate TeV gamma-ray source (Abramowski et al., 2011) and a counterpart is yet to be identified at other wavelengths.

HESS J1731–347 is known to be accelerating leptons beyond TeV energies due to the detection of non-thermal X-rays (Tian et al., 2008, 2010; Bamba et al., 2012). Thus, like IC 443 and W44 (Ackermann et al., 2013), HESS J1731–347 may plausibly also accelerate hadrons beyond TeV energies. Indeed, gamma-ray emission like that seen with HESS can be produced from cosmic-ray (CR) hadron interactions with molecular gas (hadronic production), so knowledge of the gas distribution may help to distinguish between this and a competing mechanism for gamma-ray production, inverse Compton scattering of photons by electrons (leptonic production).

Fukuda et al. (2014) argue that the HESS J1731–347 SNR is associated with a void in atomic 3 kpc-expanding Arm gas at a distance of 5.2–6.2 kpc (line of sight velocity $\sim -85 \text{ km s}^{-1}$). Their analysis of the surrounding HI and CO emission could plausibly identify a large proportion of the gas-mass required for a hadronic gamma-ray production mechanism to be consistent with observations, but the authors argue that such a scenario would still include a $\sim 20\%$ leptonic contribution to the total gamma-ray flux (much of this in the southern region of the remnant).

Certainly, upper limits placed on GeV emission using Fermi-LAT data (Yang et al., 2014) seem to disfavour a hadronic model for gamma-ray production. However, a hadronic model may still be plausible given the potential effects of cosmic ray hadron diffusion into dense gas clumps, as suggested by Fukuda et al. (2014). In this model, the highest energy cosmic rays have access to a larger amount of target material (e.g. Gabici et al. 2009).

We used the Mopra radio telescope to survey the HESS J1731–347 (and HESS J1729–345) region at 7 mm wavelengths, targeting the CS(1-0) line to trace dense molecular gas which may play a role in a hadronic gamma-ray production scenario. We simultaneously recorded emissions of several other warm gas tracers.

2. Observations & Analysis

The field displayed in Figure 1 was surveyed in March 2011, April 2012, November 2013 and May 2014 using the 22 m Mopra radio telescope, located ~ 450 km northwest of Sydney, Australia ($31^\circ 16' 04'' \text{S}$, $149^\circ 05' 59'' \text{E}$). The 7 mm spectrometer configuration and data reduction techniques were the same as those presented in Maxted et al. (2013).

Mopra mapping data have a spacing between scan rows of $26''$. The velocity resolution of the 7 mm zoom-mode data is $\sim 0.2 \text{ km s}^{-1}$. The beam FWHM and the pointing accuracy of Mopra at 7 mm are $59 \pm 2''$ and $\sim 6''$, respectively (Urquhart et al., 2010). The Mopra spectrometer, MOPS, is capable of recording sixteen tunable, 4096-channel (137.5 MHz) bands simultaneously when in ‘zoom’ mode, as used here.

The exposure varies over the mapped field, with 1σ noise levels generally within the range 0.04–0.08 K, but exceeding 0.1 K for $\sim 1\%$ of map pixels due to bad weather. To adjust for this, a

conservative threshold of 4.5σ , calculated separately for each pixel, was placed on maps to ensure false detections were not included in images.

Column densities were generated from CS(1-0) maps by applying the procedure presented in Maxted et al. (2012). Eq. 9 of Goldsmith & Langer (1999) was used to convert CS(1-0) integrated emission into CS(J=1) column density. CS(1-0) emission was assumed to be optically thin unless a detection of C³⁴S(1-0) emission was present, in which case optical depth was estimated assuming a CS-C³⁴S ratio of 22.5. To convert CS(J=1) column density into total CS column density and subsequently H₂ column density, a temperature of 20 K and a CS abundance relative to H₂ of 10^{-9} (Frerking et al., 1980) were assumed, respectively. Systematic effects due to these two assumptions are expected to be the largest contributor to the uncertainty in results, with molecular abundance possibly varying by an order of magnitude (Maxted et al. 2012 and references therein). Column density images of regions where optical depth was calculated were smoothed by a Gaussian with a width of $2'$ (two 7 mm Mopra beam-widths) to smooth the boundary between optically thick and thin analyses.

3. Results & Discussion

As displayed in Figure 1, CS(1-0) clumps were discovered at three velocity ranges towards the HESS J1731–347/HESS J1729–345 field corresponding to three Galactic arms: the 3 kpc-expanding arm, the Norma-Cygnus arm and the Scutum-Crux arm. The critical density for emission of the CS(1-0) line is $\sim 10^4 \text{ cm}^{-3}$, so Figure 1 highlights regions containing gas of a similar or higher density.

3.1 3 kpc-expanding Arm

Dense gas traced by CS(1-0) emission at ~ 6 kpc (line of sight velocity $\sim -85 \text{ km s}^{-1}$, top of Figure 1) probably corresponds to the 3 kpc-expanding arm (Vallee, 2008; Fukuda et al., 2014). HESS J1731–347 is believed to be associated with gas at this distance/velocity, however no link has been established between the northern source HESS J1729–345, and either HESS J1731–347 or gas at this velocity. Dense gas lies outside the border of HESS J1729–345 and although $\sim 4 \times 10^4 M_{\odot}$ was traced at this velocity, only $\sim 10^3 M_{\odot}$ is coincident with the gamma-ray emission (at a 4σ level).

Although $\sim 6.4 \times 10^4 M_{\odot}$ of atomic and molecular gas was previously traced towards HESS J1731–347 using the HI and CO(1-0) lines (Fukuda et al., 2014), CS(1-0) emission was not detected towards this source, suggesting an absence of dense ($\sim 10^4 \text{ cm}^{-3}$) gas detectable at a level above antenna intensity 0.04-0.08 K. This may disfavour (although not strictly rule-out) the notion that clumps of dense gas are having an effect on the high energy gamma-ray spectrum in a hadronic scenario. Specifically, diffusion into dense gas has been suggested to allow the highest energy cosmic ray hadrons to access more target material than their lower energy counterparts in the case of RXJ1713.7–3946 (Zirakashvili & Aharonian, 2010; Inoue et al., 2012; Maxted et al., 2012) and such scenarios should be investigated further for HESS J1731–347. We note that so-called ‘dark’ molecular gas (Wolfire, 2010) may exist towards the region (untraced by HI, CO and CS) and this may also affect the gamma-ray spectrum.

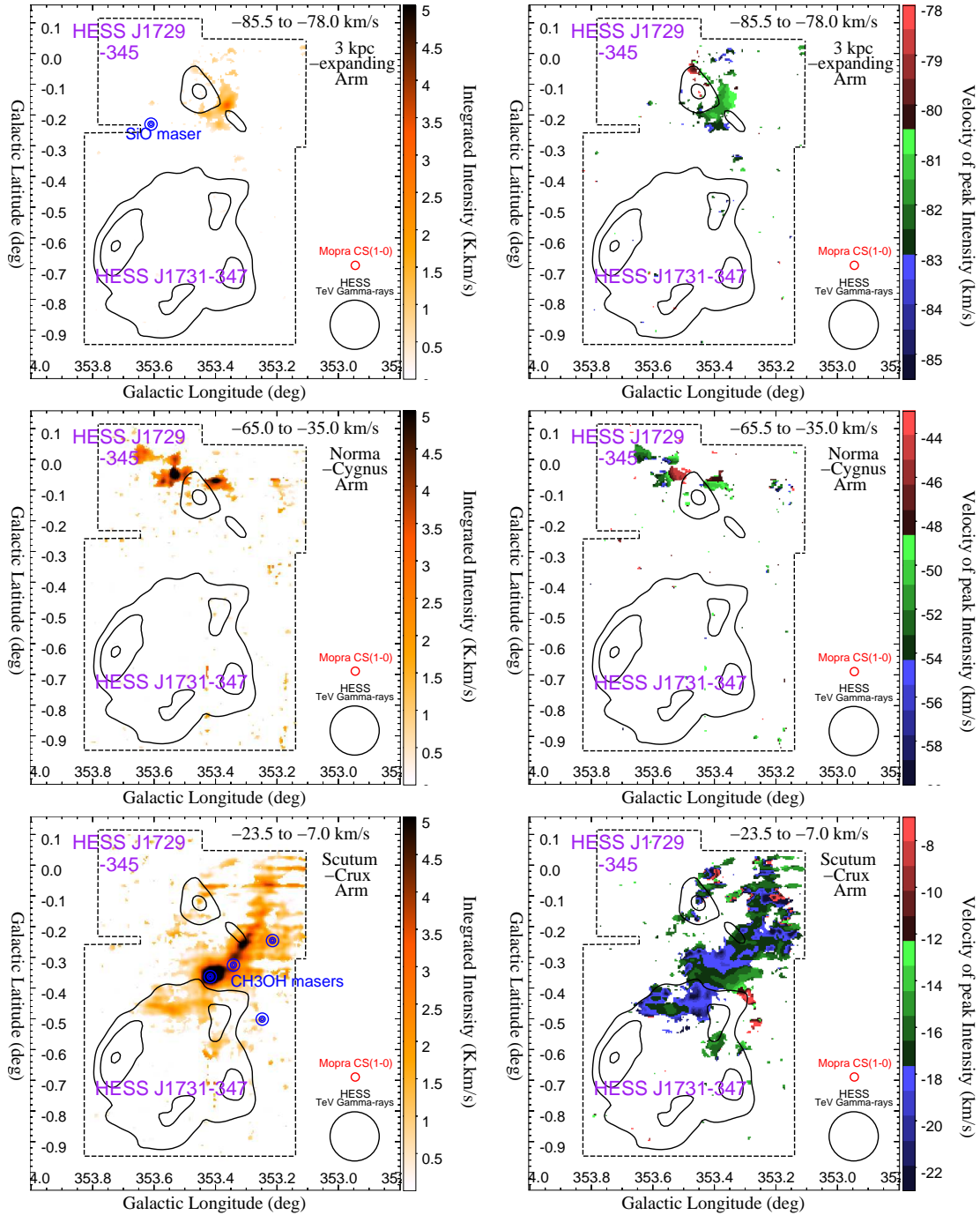


Figure 1: Mopra CS(1-0) integrated intensity (left-side) and velocity centroid (right-side) images of 3 velocity-intervals (range indicated) of CS(1-0) emission, with overlaid 4, 6 and 8 σ HESS TeV gamma-ray emission contours (Abramowski et al., 2011). The Mopra CS(1-0) and HESS TeV gamma-ray beam sizes are indicated in each picture. Exposure varies across the field (represented by the dotted line), so these images have been thresholded at a non-constant level corresponding to a signal-noise ratio of 4.5.

We also note the Mopra detection of SiO(1-0,v=2) emission at line of sight velocity $\sim -85 \text{ km s}^{-1}$ towards the location of the IR star OH 353.61–0.23 (Sevenster et al., 1997), which is not expected to be related to either of the HESS TeV gamma-ray sources.

3.2 Norma-Cygnus Arm

Dense gas traced by CS(1-0) emission at $\sim 5 \text{ kpc}$ (line of sight velocity $\sim -55 \text{ km s}^{-1}$, centre images of Figure 1) probably corresponds to the Norma-Cygnus arm (Vallee, 2008). Although CS(1-0) emission traces $\sim 10^5 M_{\odot}$ of dense gas, no significant clumps are coincident with HESS J1731–347, while $\sim 5 \times 10^3 M_{\odot}$ are coincident with HESS J1729–345 gamma-ray emission (at a 4σ level).

3.3 Scutum-Crux Arm

Dense gas at $\sim 3.2 \text{ kpc}$ ($v_{LSR} \sim -23.5 \rightarrow -7.0 \text{ km s}^{-1}$, bottom of Figure 1) may be a component of the Scutum-Crux arm (Vallee, 2008; Abramowski et al., 2011). This CS(1-0) clump harbours the HII region, G353.42–0.37, which was exploited to place a lower limit of $\sim 3.2 \text{ kpc}$ on the HESS J1731–347 SNR in previous absorption studies (Tian et al., 2008; Abramowski et al., 2011). Towards G353.42–0.37 Mopra recorded detections of C³⁴S(1-0), CH₃OH(7-6), HC₃N(5-4) and SiO(1-0) emission at velocities consistent with the CS(1-0) emission, suggesting a warm, dense and shocked environment such as that commonly associated with star-formation or gas irradiated/warmed by stellar activity. Three other CH₃OH(7-6) detections were also detected (see bottom of Figure 1). Two at $353.34^{\circ} - 0.33^{\circ}$ and $353.21^{\circ} - 0.25^{\circ}$ have no clear counterparts, but a detection at $353.25^{\circ} - 0.50$ possibly corresponds to a millimetre continuum source (BGPS G353.216-00.246, Rosolowsky et al. 2010). We note that the velocities of the four CH₃OH(7-6) emission lines match the velocities of the coincident CS(1-0) clumps (see Figure 1, details to be presented in a later publication). The dense gas has a varied velocity structure between -23.5 and -7 km s^{-1} , suggesting that it may be either composed of clumps with a range of local velocities or clumps spatially-distinct from one another (with the distance reflected in rotation velocity). No clear correspondence between velocity features and gamma-ray sources are observed.

Analyses of the CS(1-0) emission line reveal $\sim 5 \times 10^5 M_{\odot}$ of dense molecular gas, $\sim 5 \times 10^4 M_{\odot}$ of which overlaps the northern half of HESS J1731–347, while $\sim 6 \times 10^3 M_{\odot}$ overlaps HESS J1729–345.

4. Summary and Future Work

We detect dense molecular gas towards the HESS J1731–347/HESS J1729–345 region using the CS(1-0) emission line, but we do not detect CS(1-0) emission coincident with HESS J1731–347 at the currently-favoured velocity ($\sim -85 \text{ km s}^{-1}$) in this survey. We discover dense molecular gas towards and around HESS J1729–345 at three separate velocities. Despite the existence of coincident masses of $\sim 10^3 M_{\odot}$, we are unable to identify an association between the gas and the HESS J1729–345 gamma-ray emission.

References

- Ackermann, M., Ajello, M., Allafort, A., et al., 2013, *Science*, 339, 807
- Abramowski, A., Acero, F., Aharonian, F., et al., 2011, *A&A*, 531, A81
- Aharonian, F., Akhperjanian, A. G., Barres de Almeida, U., et al., 2008, *A&A*, 477, 353
- Bamba, A., Puhlhofer, G., Acero, F., et al., 2012, *ApJ*, 756, 149
- Frerking, M., Wilson, R., Linke, R. & Wannier, P., 1980, *ApJ*, 240, 65
- Fukuda, T., Yoshiike, S., Sano, H., et al., 2014, *ApJ*, 788, 94
- Gabici, S., Aharonian, F. & Casanova, S., 2009, *MNRAS*, 396, 1629
- Goldsmith, P. F. & Langer W. D., 1999, *ApJ*, 517, 209
- Inoue T., Yamazaki R., Inutsuka S. & Fukui Y., 2012, *ApJ*, 744, 71
- Maxted, N. I., Rowell, G. P., Dawson, B., et al. 2012, *MNRAS*, 419, 251
- Maxted, N. I., Rowell, G. P., Dawson, B., et al. 2013, *PASA*, 30, 14
- Rosolowsky, E., Dunham, M., Ginsburg, A., et al., 2010, *ApJS*, 188, 123
- Sevenster, M. N., Chapman, J. M., Habing, H. J. et al. 1997, *A&A*, 122, 79
- Tian, W. W., Leahy, D. A., Haverkorn, M. & Jiang, B., 2008, *ApJ*, 477, 353
- Tian, W. W., Li, Z., Leahy, D. A., et al. 2008, *ApJ*, 477, 353
- Urquhart, J., Hoare, M., Purcell, C., et al., 2010, *PASA*, 27, 321
- Vallee J, 2008, *ApJ*. 135, 1301
- Wolfire , M., Hollenbach, D. & McKee, C., 2010, *ApJ*, 716, 1191
- Yang, R., Zhang, X., Yuan, Q. & Liu, S., 2014, *A&A*, 567, 23
- Zirakashvili V. & Aharonian F., 2010, *ApJ*, 708, 965